On the Dynamics of Global Temperature

David R.B. Stockwell*

August 2, 2011

Abstract

In this alternative theory of global temperature dynamics over the annual to the glacial time scales, the accumulation of variations in solar irradiance dominates the dynamics of global temperature change. A straightforward recurrence matrix representation of the atmosphere/surface/deep ocean system, models temperature changes by (1) the size of a forcing, (2) its duration (due to accumulation of heat), and (3) the depth of forcing in the atmosphere/surface/deep ocean system (due to increasing mixing losses and increasing intrinsic gain with depth). The model can explain most of the rise in temperature since 1950, and more than 70% of the variance with correct phase shift of the 11-year solar cycle. Global temperature displays the characteristics of an accumulative system over 6 temporal orders of magnitude, as shown by a linear f^{-1} log-log relationship of frequency to the temperature range, and other statistical relationships such as near random-walk and distribution asymmetry. Over the last century, annual global surface tempera-

*davids99us@gmail.com

ture rises or falls $0.063 \pm 0.028 C/W/m^2$ per year when solar irradiance is greater or less than an equilibrium value of $1366 W/m^2$ at top-of-atmosphere. Due to an extremely slow characteristic time scale the notion of 'equilibrium climate sensitivity' is largely superfluous. The theory does not require a range of distinctive feedback and lag parameters. Mixing losses attenuate the effectiveness of greenhouse gasses. Most recent warming can be explained without recourse to increases in heat-trapping gases produced by human activities.

1 Introduction

An accumulating body of evidence showing high sensitivity of global temperature to solar variations, accounting for more than half of global warming since the mid 20th century Douglass and Clader [2002], Shaviv [2008], Scafetta and West [2007], Scafetta [2009, 2010a,b], and the recent (2003 – 2011) flat warming/cooling rate of $0.1 \pm 0.2 W/m^2$ ocean heat content anomaly instead of the frequently-cited, large, positive computed radiative imbalance of $0.6 \pm 0.3 W/m^2$ Knox and Douglass [2010], demands an explanation. The absence of a known mechanism to explain why Earth's temperature may be 'mysteriously hypersensitive to solar variations' Scafetta et al. [2009], Duffy et al. [2009] blocks the acceptance of these empirical results Lockwood and Fröhlich [2008].

Another related problem is the range of estimates of climate sensitivity between climate models IPCC [2007] and natural experiments Idso [1998], natural cycles Scafetta [2010b], Douglass and Clader [2002], the Pinatubo event Douglass and Knox [2005], Douglass et al. [2006b], Bender et al. [2010], and temperature fluctuations Stott et al. [2003], Lindzen and Choi [2009], Spencer and Braswell [2010], Dessler [2010]. These issues, together with the difficulty of reducing the range of estimates of the sensitivity of the system to CO_2 doubling to less than an order of magnitude IPCC [2007] suggests a fundamental gap in our understanding of climate sensitivity.

Global temperature variations are conventionally thought of as the interaction of different types of forcings and feedbacks over different time scales: fast, medium and slow depending on type, water vapour, GHGs, and ice-sheet albedo Hansen et al. [2011]. Model sensitivity ranges from $0.75C/W/m^2$ to $8C/W/m^2$ and greater for long term equilibria Stern [2005]. General Circulation Models (GCMs) attempt to represent the complexity of these physical relationships and values, both measured and presumed.

Natural and modeled systems contain a mix of fast and slow equilibrating components. They have a crucial difference. If fast, then continued forcing at the same average level does not cause any additional warming; forcing is directly related to response. If slow, constant high levels can cause ongoing warming until equilibrium is reached. In the slow case, the forcing cannot be directly related to the response, and requires a slightly more complex model, here an autocorrelated (AR) recurrence equation or matrix. We claim here (1) the slow, equilibrium component is largely due to the simple, physical, accumulation of heat; (2) the accumulative mechanism is responsible for high sensitivity to solar radiation, and consequently; (3) insufficient consideration of slow dynamics has lead to errors and underestimation of the contribution of solar forcing to climate change.

Energy Balance Models (EBMs) are simple models of the temperature response of a body to energy coming in and going out, in this case the Earth Knox and Douglass [2010]. We will consider the conjecture (called the 'Accumulation Theory of Climate Change') that accumulated energy provides a parsimonious and physically motivated explanation for a wide range of climate observations. The development of the theory draws on notions from control theory Stubberud et al. [1994] and the electronic integration amplifier. In the first section, we show evidence the theory explains, and the physical representation of near-random walk behavior of the Earth's temperature. We then explain the inverse relationship of temperature variance to the time scale (f^{-1}) over at least six orders of magnitude.

This approach is also justified by cointegration theory, wherein variables can only be related if they have the same long-run behaviour, i.e they are both stable (stationary or zero trend) or both unstable (non-stationary or trending). Integration order $I(n)$ is the number of differentiations n required to make the variable stable. It has been shown that while solar intensity is $I(0)$, global temperature requires one differentiation to become stable, and is, therefore, $I(1)$ Beenstock and Reingewertz [2010]. Order difference is like apples and oranges; the correct approach is to bring them to the same order by integrating solar intensity before regressing with global temperature, as we do here.

At the contemporary time scale, solar irradiance since 1950 has been above average Usoskin et al. [2003], Solanki et al. [2004]. We show that accumulation of the above average solar isolation can explain the majority of the magnitude and phase of temperature variations from 1950 to the present. The AR coefficient of atmospheric temperature increases with decreasing height, increasing linearly with increasing density, from 0.2 to 0.5 in the upper and lower troposphere, to 0.9 at the surface and more in the deep ocean. The graduated AR system creates multiple characteristic decay times represented by a recurrence matrix model.

The use of a matrix recurrence formula to analyse climate sensitivity in the climate system is a new approach, growing out of previous work on stochastic models and the spectral scaling of climate variability Vjushin et al. [2002], Stockwell [2006], Koutsoyiannis and Cohn [2008], and empirical studies of derivatives and integrals of tropical ocean indices and multi-decadal warming trends McLean et al. [2009], Stockwell and Cox [2009].

2 Observations

2.1 Paleoclimatic Time Scale

A good theory should explain all the available observations with as few parameters as possible. The Earth's temperature record spans over 10^6 to 10^{-2} years. Global temperature data sets ranging over the 30 years monthly variations of satellite records, to 150 year surface temperature records, 1000 year proxy climate records, and the 800,000 years EPICA ice core record. The variance or range or spectral power of these data varies with frequency f (or wavelength f^{-1}) (Fig. 1).

The time series needs some preparation due to spectral biases. The EPICA record was aggregated to 1000-year means and dividing by 4 to account for polar bias. The proxy records Loehle [2007], Moberg et al. [2005] were aggregated to 20 year means.

A spectral plot of the data sets (Fig 1) shows a single, linear relationship (solid grey line) with decline of almost f^{-1} (dashed grey line). Remarkably, the standard deviation (SD) of temperature over 6 orders of magnitude appears to be proportional to the log of the wavelength:

$$SD(t) \propto log(wavelength).$$

For example, if the standard deviation (σ) is 0.1C at the scale of one year, then natural variation over 10 years will be 0.23C, 100 years will be 0.46C, 1000 years will be 0.69C and over the million years, 1.38C. These figures are consistent with a range of around 5C for glacial-interglacial transitions. The power spectrum may deviate from the linear relationship at the maximum and minimum ends as shown.

Low total variation in solar irradiation (TSI) is available to generate such such temperature variations. TSI is around $1366 W/m^2$ at the top of atmosphere, but the geometry of the globe and an average albedo of 30% reduces surface TSI to 17% or $235 W/m^2$. Variations in TSI over the 11 year solar cycle typically do not exceed 0.1% or $0.24 W/m^2$ at the surface. The increase in TSI since the last century is about $0.28 W/m^2$, while variation in TSI varies no more than 0.2% or $0.5 W/m^2$ at the surface over 100,000 years due to orbital variations Lean and Rind [2001], Muscheler et al. [2007]. Geological forcing is of smaller magnitude, estimated at $0.09 W/m^2$.

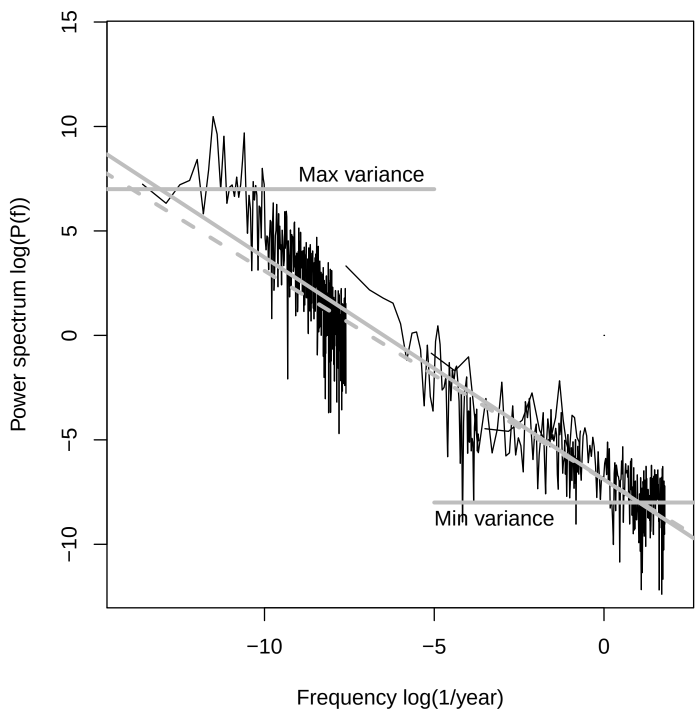

Figure 1: Power spectrum of estimates of global temperature ranging from 800K years (EPICA ice core) to the 30 years (satellite record). The line of best fit through the data (gray) does not differ significantly from the theoretically expected inverse of frequency f^{-1} found in integration amplifiers. Horizontal gray lines indicate possible maximum and minimum amplitudes at approximately 22,000 years and 1 year.

The temperature sensitivity of a black body to forcing is $0.25C/W/m^2$ to $0.3C/W/m^2$. Therefore, the direct, proportional effect of an increase in solar forcing of $0.2W/m^2$ would be only 0.05C. Conventionally, small changes in temperature launch feedbacks from water vapor, greenhouse gases and surface albedo that promote the response of the Earth's atmosphere by an order of magnitude.

In the accumulative theory, accumulation of heat in the mass of the land and ocean causes global temperature increases. Both the magnitude and the duration of a forcing determines the heat accumulated and, therefore, the temperature.

A 'back of envelope' calculation indicates that a solar forcing of $0.1W/m^2$ for 1 year transfers $3.1x10^6$ Joules of heat ($3.1x10^6$ sec in a year) to the ocean. Based on the specific heat of water (4.2 J/gK) and the number of grams in a cubic meter of water (10^6), a water column 100 m deep would warm 0.008K in one year, or 0.8K in a century. Thus, the 20th century temperature rise can be explained by the accumulation of an above average solar forcing of $0.1W/m^2$ in the ocean over the period Lean and Rind [2001, 2008].

Similarly, a forcing of $0.1W/m^2$ accumulated for 5,000 years would increase the whole ocean temperature by 4C, sufficient to account for interglacial warming.

Control systems theory provides an elegant and powerful formalism for describing such systems. The Bode plot (Fig. 2) illustrates the spectral energy (upper), and phase relationship (lower) to the frequency (or wavelength) that simultaneously provides a complete picture of the way a system

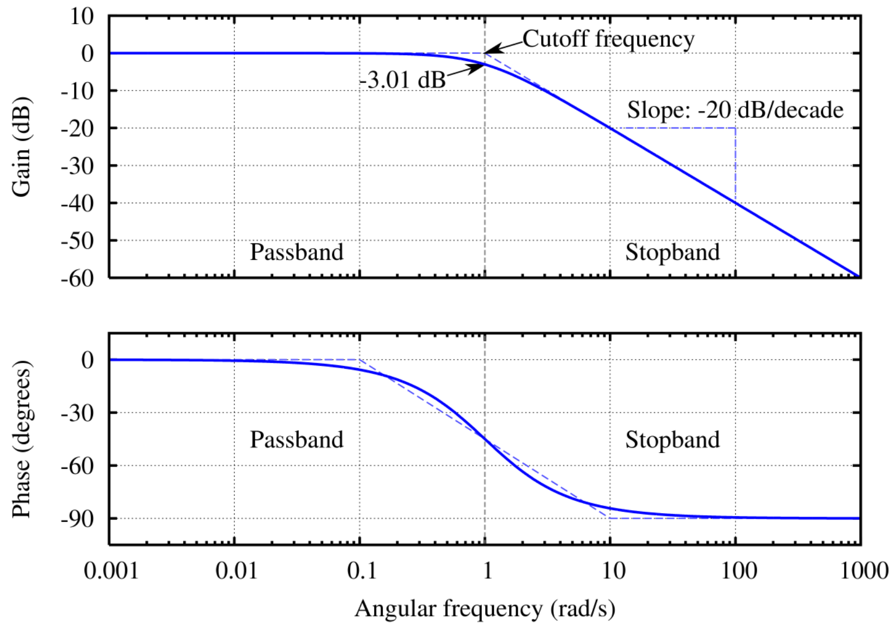

Figure 2: A Bode plot for an integrative amplifier, or low-pass filter, showing the amplification increases linearly with decreasing frequency until it reaches an amplification limit at a cutoff frequency. The phase also varies with frequency (from Wiki commons).

modifies input Stubberud et al. [1994]. The frequency response of a ideal integrator is a downward-sloping line, indicating higher gain at lower frequencies:

T1: f^{-1}

A finite accumulator has a plateau of maximum gain (Fig 2). Basic control theory shows how the function below can be obtained from the Laplace transform of the basic energy balance model (4) described in the next section Stubberud et al. [1994].

T2: $(\alpha + f)^{-1}$

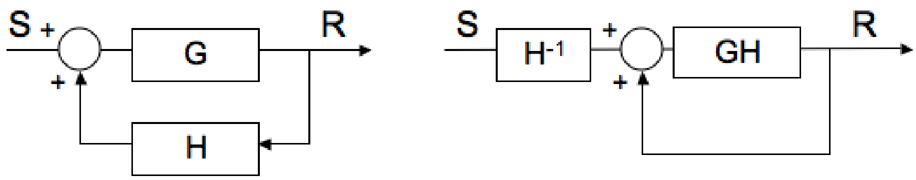

Figure 3: (A) A feedback controller with system components G and feedback H, and (B) the corresponding diagram rearranged into an integration amplifier, where the feedback is a unit loop.

T1 is a ideal integrator with an infinite gain at zero (low) frequency. T2 has finite gain via the inclusion of a small system loss. 'Reddening' is a bias of random noise towards low frequencies Roe [2009]. In comparison, random or white noise has equal power at all frequencies, producing a horizontal line on the spectral plot.

We can now explain the maximum and minimum limits to the integrator in the spectral plot of global temperature (Fig 1). The maximum response appears at about period e^{10} or 22,000 years, suggesting the limits of the temperature range. The minimum variance appears at time periods less than one year suggestive of white noise. The Earth system appears to act as an ideal integration amplifier between these time scales.

Control systems theory formalizes the notion of feedbacks (Fig. 3). The simplest loop has two transfer functions, a transient system amplification G and a feedback H summed at the control point (A). H and G are simply constants. The recurrence equation $Y_{i+1} = G(S + HY_i)$ describes one iteration around the loop:

$$Y_{i+1} = GHY_i + GS$$

An integration amplifier, the block diagram in Fig 3 (A), can be rearranged as a unit loop (B), summing output and input. Though this rearrangement, amplification is a single transfer function $\frac{1}{H} * GH$ or G embedded in an iterative sum. The two views are equivalent; feedback can be transformed into an integrating amplifier.

The example demonstrates that integration is more specific than feedback; asserting the dominant mechanism of climate change is an accumulation mechanism is a stronger claim than invoking feedbacks. For example, in classical feedback an increase in isolation of $0.1W/m^2$ produces more water vapour in the air which permits absorption of $0.2W/m^2$ of radiation. In the accumulative view, increasing humidity and temperature can be regarded as the accumulated stock of heat.

2.2 Recent Warming

The conventional view of global warming is that there is no plausible explanation for the rise in temperature since 1950 other than the heat-trapping effects of human emissions of greenhouse gasses IPCC [2007]. We explore a model of accumulated solar radiation denoted $\Sigma Solar$ (or CumSolar on the Figures) Lean [2001], also a sunspot series due to uncertainty in the solar irradiance satellite composites Scafetta [2009].

Exhaustive search for the equilibrium value was optimized on the correlation of accumulated monthly irradiance (and sunspots) with HadCRU temperature from 1950 and to present. The zero point was 1365.9 W/m^2 and 21 monthly sunspots; temperature is generally rising above and generally falling below these values. The equilibrium value was subtracted from the solar irradiance series before accumulation, producing $\Sigma Solar$.

Figures 4, 5, 6, and 7 show the linear regressions of $\Sigma Solar$ against global temperature datasets. The $\Sigma Solar$ variable is highly significant and accounts for more than 60% (blue) and 70% (red including volcanics) of the variation (Fig. 7). By comparison, the direct irradiance has little correlation (R2<0.1) (orange). Solar sunspot counts gave similar results.

An additional regression including a time term provided the opportunity for another trending factor, such as increasing concentrations of greenhouse gasses, to explain the trend. If the trend term was significant, then the relative contribution of $\Sigma Solar$ to the warming trend would be estimated by subtracting the residual trend from the overall trend. The residual trend term was not significant in any of the data sets. The accumulated radiance was 128 W/m^2 during the 58 years since 1950, representing an average solar forcing of 0.18 W/m^2 at the top of the atmosphere (TOA) (i.e. 128/58 years/12 months).

The $\Sigma Solar$ variable also has the correct phase relationship with temperature, as shown by the peak of the cross-correlation at zero lag (Fig. 8). The volcanics and direct sun spots have low, lagged correlation. Changes in ocean temperatures lead land temperatures by one year, indicative of an ocean-controlled system.

Fig. 9 illustrates the main assumed atmospheric forcings from the GISS general circulation model (GCM) (as listed in the file RadF.txt) Hansen et al. [2011] and brought up to date from 2003: well mixed green house

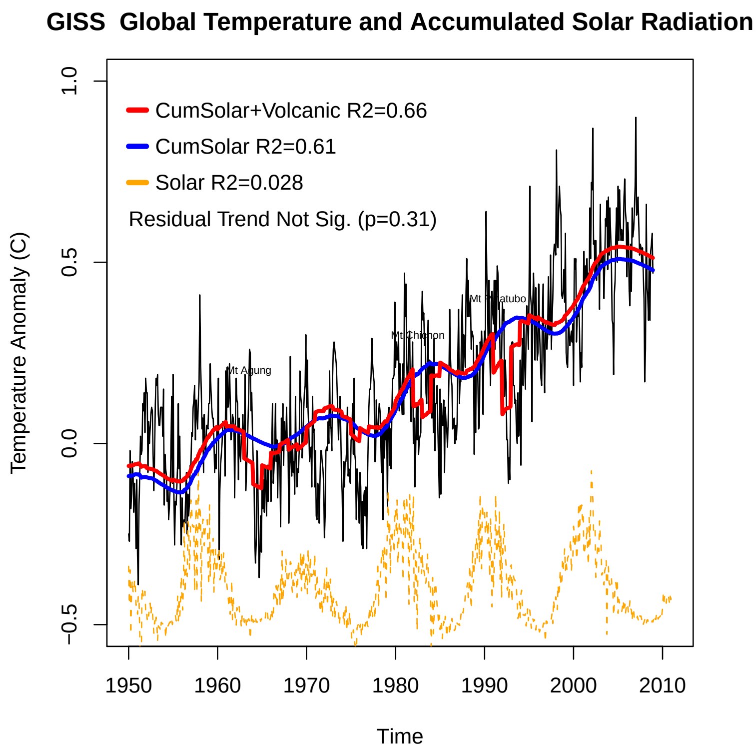

Figure 4: Cumulative solar irradiance (blue) and volcanic forcing (red) is highly correlated with GISS sea surface global temperature and explains the trend in temperature since 1950. The direct solar irradiance (orange) is uncorrelated with temperature.

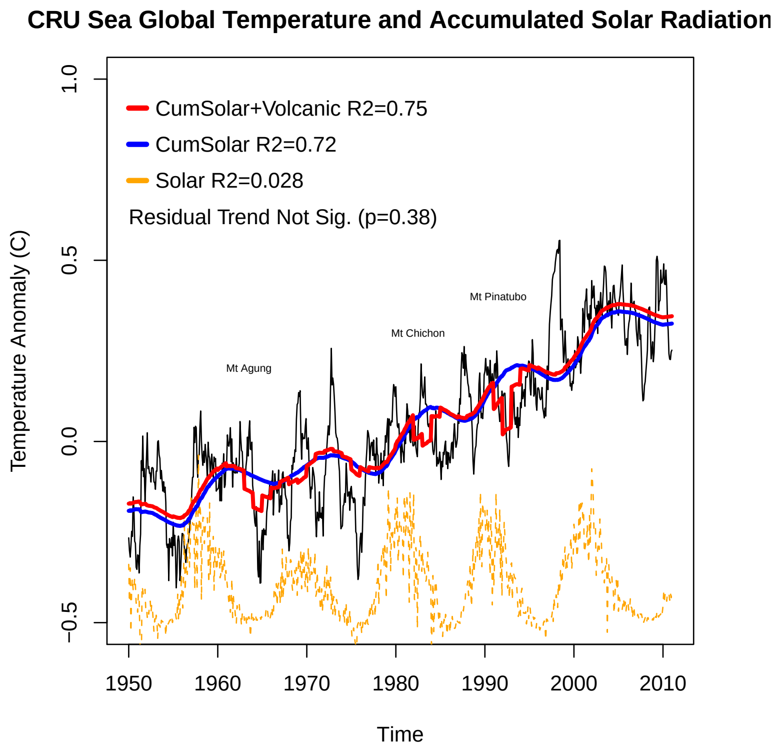

Figure 5: Cumulative solar irradiance (blue) and volcanic forcing (red) is highly correlated with HadSST sea surface global temperature and explains the trend in temperature since 1950. The direct solar irradiance (orange) is uncorrelated with temperature.

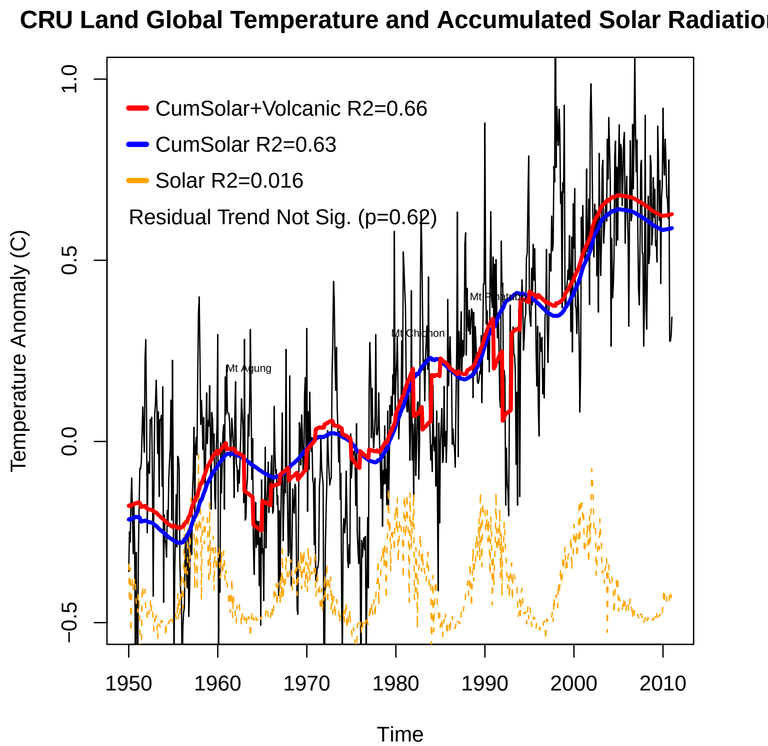

Figure 6: Cumulative solar irradiance (blue) and volcanic forcing (red) is highly correlated with HadLST land surface global temperature and explains the trend in temperature since 1950. The direct solar irradiance (orange) is uncorrelated with temperature.

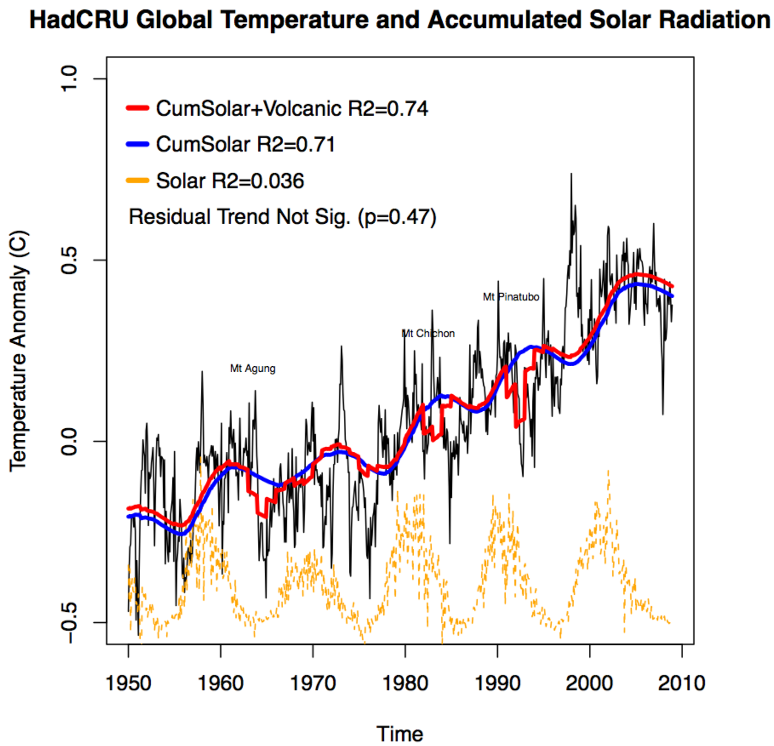

Figure 7: Cumulative solar irradiance (blue) and volcanic forcing (red) is highly correlated with HadCRU global temperature and explains the trend in temperature since 1950. The direct solar irradiance (orange) is uncorrelated with temperature.

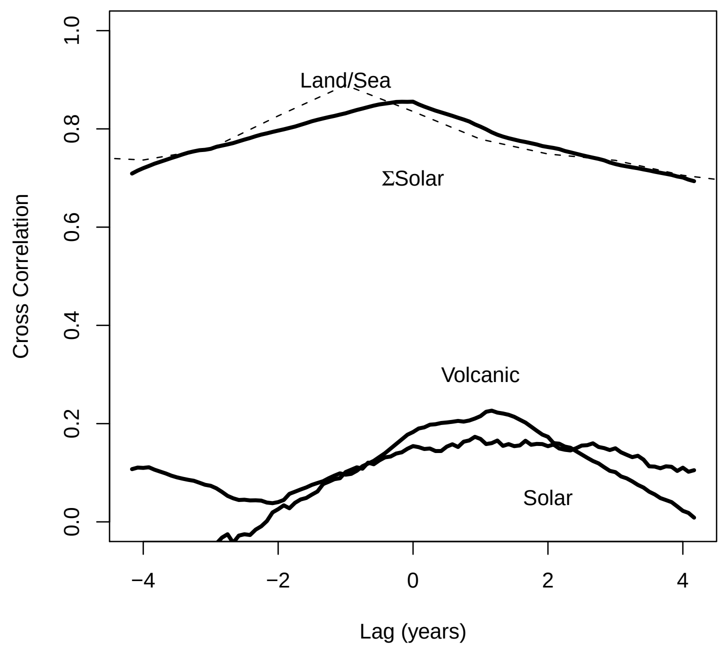

Figure 8: The cross correlation relationships showing the high correlation and correct phase of the accumulated solar radiance. The volcanics are lower correlation and lagged while the direct solar irradiance has very low, lagged correlation. Also shown is the one year lead of ocean over land temperatures (dashed).

gasses, W.M_GHGs, which warmed the Earth about 1.3C, stratospheric aerosols (volcanic) StratAer, and reflective aerosols ReflAer which cooled it about 0.7C. Regression without $\Sigma Solar$ replicates the assumed contribution of W.M_GHGs and aerosols in the GISS dataset (dashed lines in Fig.9).

The contribution of W.M_GHGs drops to less than half with $\Sigma Solar$ in the regression (red arrow). Thus, a combination of forcings with lower estimates of CO_2 sensitivity and higher solar contribution would be consistent with both the rise in global temperature, and the flattening of temperatures and ocean heat uptake in the last decade Loehle [2009], Douglass and Knox [2009], Knox and Douglass [2010].

2.3 Climate cycles and other effects

The most prominent climate cycles are the solar (Schwabe) cycle averaging 11 years, the Pacific Decadal Oscillation (PDO) and the Atlantic Meridional Oscillation (AMO) with a quasi-periodicity of around 60 years, and Milankovitch cycles of period around 100,000 years related to the transition between ice ages.

The accumulation theory suggests that the amplitude of the cycles should be directly related to their duration, as appears to be the case (Fig 1). Control theory also predicts peak power at $2\pi\tau$ or about six times the characteristic decay time Stubberud et al. [1994] related to the 11 year solar cycle and the 60 year PDO and AMO oscillations.

Further, control theory shows that the start of the maximum plateau

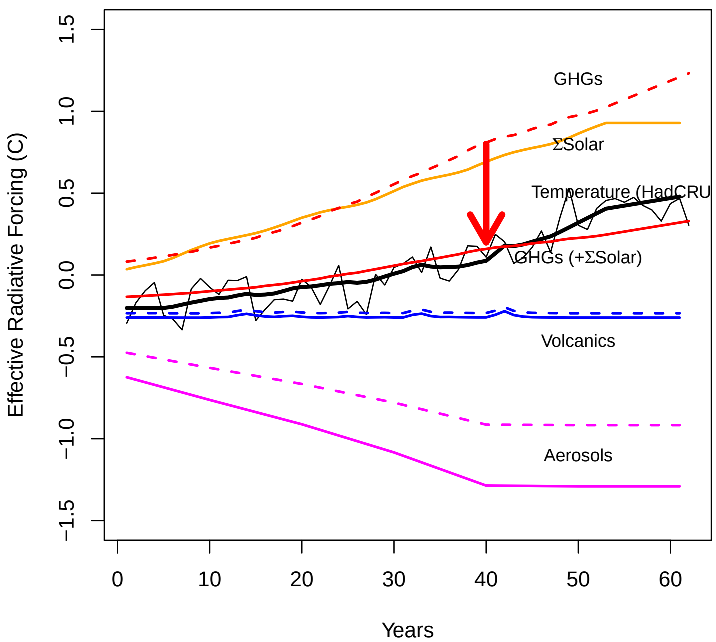

Figure 9: Climate forcings and their contributions to temperature change from the GISS forcing estimates. Regression of GHGs (red) aerosols (purple) and stratospheric aerosols (volcanics - blue) with the observed increase in temperature (black and gray) replicates the assumed contributions in Hansen et al. [2011]. Inclusion of cumulative solar (orange) in the regression decreases GHG contribution by more than half and increases the aerosol contribution.

region in the spectral plot in Fig. 1 is at 2π times the characteristic decay time. Thus, the dominant decay time of the system is around 3500 years, which would give an AR coefficient of $a = 0.99971$ – extremely close to a random walk but still stationary (stable).

Further evidence in of the model is controlled output and uncontrolled input, as seen in assymetric temperature changes. Asymmetry is indicated when the mean of differences exceeds the median of the differences. The mean of the EPICA data is 0.01C, greater than the median of -0.07C. In HadCRUT, the mean is 0.005C, greater than the median of 0.003C. In TLT, the mean is 0.002C, greater than the median of -0.009C, indicating asymmetry and hence output control.

The accumulation theory does not ignore added forcing, such as interactions between solar emanations and the Earth's magnetic field such as modification of cloud albedo by high-energy particles Svensmark [2007]. Rather, the accumulation theory defines the basic functioning of the system, while indirect solar effects, cloud albedo variations, and aerosols only serve to change the intensity of radiative inputs to the system. Small forcing over long periods may control the timing of cycles.

3 The Models

3.1 Recurrence Models

A random walk is a mathematical formalisation of trajectories that accumulate successive random shocks. A non-stationary random walk has no tendency to return to a fixed value. More generally, mean-reverting series are modelled with first-order autoregression models (ARM) (e.g. Tol and Vellinga [1998], Breusch and Vahid [2008]):

$$T_n = a\ T_{n-1} + S_{n-1} + \epsilon$$

Here a is the autocorrelation coefficient, S_n is the deterministic radiative forcing at times n due to any factor: solar variations, increases in greenhouse gases, aerosols, and volcanic eruptions, and ϵ is the random error. We assert that the recurrence equation models not only the errors but also the response of the system itself, particularly when the response time is long. This approach may be too elementary for real system modelling and prone to diagnostic bias Foster et al. [2009] stemming from several decay times, particularly long-term ones (>100 years) Stern [2005]. A recurrence matrix formula introduces multiple time scales. A physical system with random-walk behavior has no tendency to return to an equilibrium value, effectively having an infinite characteristic decay time. A value of $a < 1$ ensures its eventual return. A good way to assess the behavior of these equations is to examine the response to a constant step forcing S as shown in Fig 10. When the autoregession term a is zero, the response follows the step. If the $a = 1$ then the response diverges to plus infinity.

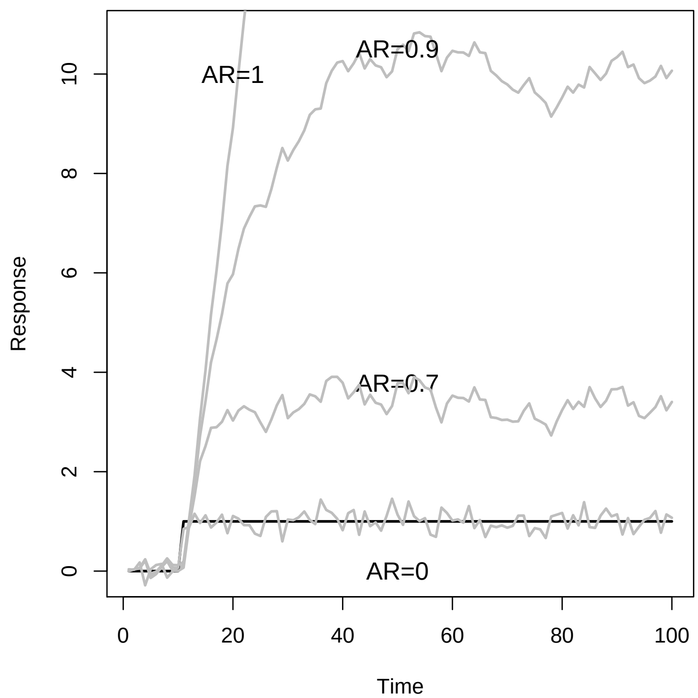

Figure 10: The increasing response to a step forcing (black) of magnitude 1 by recurrence equations with increasing AR value and random noise, for AR values of 0, 0.7, 0.9 and 1.

We can calculate the trajectory of a recurrence equation by summing consecutive terms. The divergent behavior of the random walk in Fig 10 is due to the ever increasing sum of the constant level forcing S, as follows:

$$T_n = T_0 + \sum_{t=0}^{n} (S + \epsilon_t)$$

An equation with AR of less than one (e.g. $a = 0.7$) increases in a decreasing exponential to a maximum value. A higher AR (e.g. $a = 0.9$) results in a higher but still limited equilibrium level(Fig 10). The size of this response to the step forcing is indicative of the intrinsic gain.

Simplifying the equation by dropping the ϵ, the pattern of the recurrence equation which after n steps can be expressed as the summation shown below.

$$T_n = a(...(aT_0 + \frac{S}{C})...) + \frac{S}{C} = a^n T_0 + \frac{S}{C} \sum_{t=0}^{n} a^t$$

It is clear that when $0 < a < 1$, as $n \to \infty$ then $a^n T_0 \to 0$ and the limit of the geometric series goes to $\tau = \frac{1}{1-a}$. The single parameter τ governs both the rate of the rise and the height of the final equilibrium, so that the characteristic decay time or rise time, the intrinsic gain and the amplification are equivalent. As an example, the 5C range of glacial-interglacial transitions may be simulated by feeding random energy (mean=0, $\sigma = 0.1C$) into a recurrence equation with an autocorrelation coefficient of nearly one.

From the analysis above, there is a clear meaning of AR as fractional retention. A system with $a = 1$ represents a ideal accumulator with no losses. The value $1 - a$ is the loss or leakage at each time step. In the case of a real energy balance model, the equation describes an object absorbing heat and increasing temperature in response to radiative forcing, where the loss is proportional to the current temperature.

3.2 Energy Balance Models

We now derive the recurrence model from the solutions to differential equations in a zero-dimensional energy balance model (EBM). A useful conceptual model of an EBM is a fluid surge tank, used to moderate pressure and flow in hydraulic systems. S is an unregulated input, C a tank capacity with fluid level T, and F a regulated output. When the surge tank receives a sudden inflow, fluid volume in the tank accumulates and the level T rises. Output F increases proportional to T and the fluid level eventually stabilizes. The model responds at an impulsive forcing with exponential decay, and rises to a new level T when the forcing persists.

The set of equations below describe a standard EBM Spencer and Braswell [2008]: ΔS is the change in short-wave radiation into the Earth's atmosphere, ΔF is the change in longwave radiation leaving the atmosphere, and ΔT is the change in global-mean average temperature at the Earth's surface and T:

$$\Delta T = \lambda \Delta F \tag{1}$$

$$C\frac{dT}{dt} = (S - F) \tag{2}$$

$$\frac{dT}{dt} + \frac{T}{\lambda C} = \frac{S}{C} \tag{3}$$

$$T(t) = \frac{e^{\frac{-t}{\tau}}}{C} \int e^{\frac{t}{\tau}} S(t) dt \tag{4}$$

The parameter λ in (1) states that temperature and radiative forcing are proportional, with units of Kelvin per Watts per meter squared ($K/W/m^2$). The heat capacity C in (2) gives the proportional rate of change of temperature due to radiative forcing, or imbalance (S-F), with units of Joules per Kelvin (J/K). Substituting equation (1) into (2) gives the first-order ordinary differential equation (3), with a solution (4). The characteristic decay time, or rise time τ is given by $\tau = \lambda C$.

To gain greater familiarity with the solution, Fig. 11 illustrates the behaviour of (4) in response to impulse, constant, and fast and slow periodic forcing.

An impulse forcing (Fig. 11A) decays exponentially after the initial surge due to the negative exponential. Step forcing (Fig. 11B) converges to a stable, higher value. Pure integration, unaffected by exponential decay, would ramp up constantly on a step increase (thick dashed line in Fig. 11B). Short period forcing (Fig. 11C) shows amplification (but less than in Fig. 11B), and a prominent phase shift of around 90 degrees. Finally, a slower periodic forcing (Fig. 11D) shows higher amplification due to the longer period of warming.

The model produces amplification and lag, and a maximum proportional to the size and duration of the forcing and the decay properties τ of the

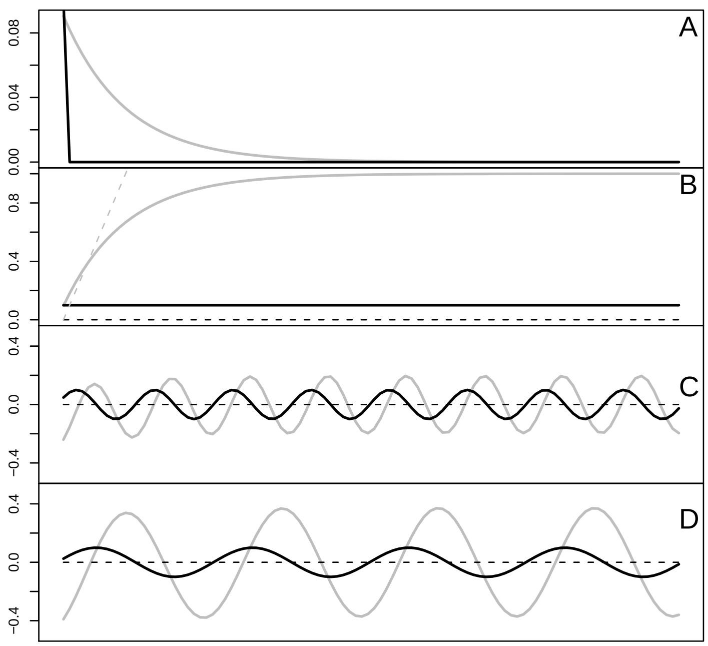

Figure 11: The response (gray) of the energy balance equation 4 to a range of forcings (black) of amplitude 0.1: (A) impulse, (B) step, (C) short periodic and (D) long periodic. Note the apparent amplification of longer period forcing exceeds the short period forcing.

system.

Equation (3) written as a first order autoregressive model (order=(1,0,0)) is:

$$T_t - T_{t-1} + \frac{T_{t-1}}{\tau} = \frac{S_{t-1}}{C} \tag{5}$$

$$T_t = a\ T_{t-1} + \frac{S_{t-1}}{C} \tag{6}$$

Note that $a = 1 - \frac{1}{\tau}$ but the exact discretization is $a = e^{\frac{-t}{\tau}}$, a source of significant bias only if the rise time is less than the sampling period (e.g. less than a year).

3.3 Linked Systems

A three-component system with levels atmosphere, surface and ocean basins that accumulate and pass heat between them is as follows:

$$\begin{bmatrix} x_i \\ y_i \\ z_i \end{bmatrix} = \begin{bmatrix} a_x & a_{yx} & 0 \\ a_{xy} & a_y & a_{zy} \\ 0 & a_{yz} & a_z \end{bmatrix} \begin{bmatrix} x_{i-1} \\ y_{i-1} \\ z_{i-1} \end{bmatrix} + \begin{bmatrix} X_{i-1} \\ Y_{i-1} \\ Z_{i-1} \end{bmatrix} \tag{7}$$

The diagonal entries in the matrix represent the persistence from one time step to another, while the off-diagonal entries represent the transfer of energy from one level to another. The matrix is in tridiagonal form, where each component communicates with the next, as in a cascade of surge tanks. As the system is at equilibrium, the matrix should also be symmetric which has interpretative and computational benefits.

The intrinsic AR coefficients (and decay rates) will match the eigenvalues of the matrix and not the values on the diagonal. In particular, the dominant eigenvalue of the recurrence matrix will be the largest value.

4 Parameterization

A linear regression can be used to estimate the parameters of the system with the form:

$$T_i = aT_{i-1} + bS_{i-1} + c$$

where a is the AR coefficient, S is the solar irradiance at the TOA, b is the effect of changes in solar irradiance on global temperature T, and c is the intercept that allows us to calculate the equilibrium value. The result of fitting the HadCRU annual temperature to the solar irradiance from Lean et.al. (2001) are as follows:

$$a = 0.89 \pm 0.04; b = 0.063 \pm 0.029C/Wm^2; c = -86.2 \pm 39; R2 = 0.8603$$

The solar effect on temperature is $0.06 \pm 0.03C/Wm^2/yr$. The volume of water that would rise by 0.06C after one year of even heating by 1Watt has a depth of 159 meters, corresponding to the midpoint depth of the tropical ocean thermocline. We can also calculate the equilibrium value of $86.2/0.063 = 1365.9Wm^2$ as found previously.

4.1 Earth Components

A standard ARIMA fitting procedure with order=(1,0,0) estimated the AR and SD parameters of natural data sets. The AR in the atmosphere (Table 1) decreases from 0.5 for the lower troposphere, to 0.2 in the upper troposphere. The AR at the surface (Table 2) is around 0.9. The AR of the EPICA data is indistinguishable from one due to limitations of the ARIMA algorithm, while the AR of the Zachos sediment core data Zachos et al. [2001] is lower than expected, probably due to data gaps. However, an estimated decay time of 3500 years from the spectral plot and the bandwidth relationship noted previously would give $a = 0.9997$.

	AR	sd1	SD	tau
UAH	0.4969	0.0276	0.1701	1.99
TLT	0.5427	0.0252	0.1654	2.19
TMT	0.2853	0.0324	0.1584	1.40
TTS	0.1328	0.0464	0.1600	1.15
TLS	0.7685	0.0120	0.2507	4.32

Table 1: Estimates of the AR coefficients and SD of atmospheric temperature data from 1979 to present.

We also note in passing that $AR \propto log(Height)$ indicating a functional relationship of AR to the density of the atmosphere, and thus to λC and τ.

According to the accumulation model, system gain increases with more

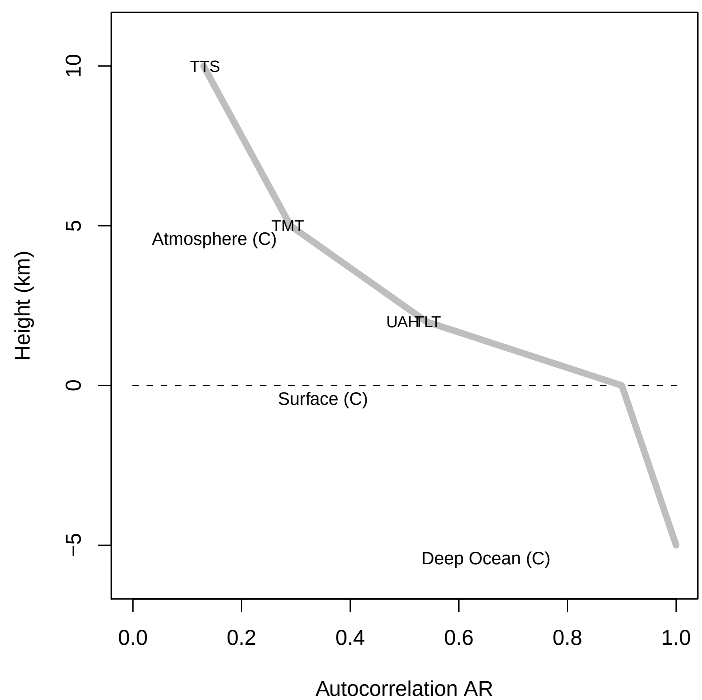

Figure 12: The AR coefficient of the global temperature series decreases with height. This is indicative of a system that loses less energy (retains more energy) per step, with increasing depth.

	AR	sd1	SD	tau
HadCRU	0.9298	0.0009	0.0998	14.25
HadSST	0.9152	0.0010	0.1004	11.80
HadLST	0.8571	0.0016	0.1689	7.00
GISS	0.9068	0.0014	0.1069	10.73

Table 2: Estimates of the AR coefficients and SD of surface temperature data from 1850 to present.

	AR	sd1	SD	tau
vosreg	1.0000	-0.0000	0.7204	480338.72
zachos	0.7415	0.0006	0.2854	3.87

Table 3: Estimates of the AR coefficients and SD of paleoclimate datasets from 800,000BC

efficient accumulation of shocks and lower rates of loss. The intrinsic gain increases with decreasing altitude, from 1 or 2 to 10 at the surface and extremely high in the deep ocean (Fig 12). Thus, system response to a forcing depends not only on (1) the size of a forcing, and (2) its duration (affecting the accumulation of heat), but also (3) the forcing depth in a system. For example, long-wave forcing of the low AR, high loss atmospheric level by GHGs would differ from shortwave solar radiation forcing the surface layers of the land and ocean. Geothermal heating in the deep ocean would have the highest intrinsic gain, due to reduced losses.

Furthermore, it is clear that the different values for climate sensitivity produced by different studies could easily result by observing of different parts of the system. Studies of short term atmospheric effects, like the Pinatubo eruption, should necessarily provide low sensitivity (e.g. 0.17 to 0.20 $C/W/m^2$ Douglass and Knox [2005]), while surface observations would yield higher values Idso [1998]. Higher sensitivity of $2K/(W/m^2)$ would result from observations of surface ocean layers, such as correlative solar estimates Scafetta [2010a], while the highest sensitivity would result from running coupled ocean GCMs over long periods due to the dominating effect of the deep ocean Hansen et al. [2011].

4.2 Climate models

Evaluation of computer simulations complements analysis of natural temperature series Koutsoyiannis et al. [2008], Douglass et al. [2008], Santer et al. [2008]. Table 4) lists the AR and SD for each GCM illustrated graphically in Fig 13, along with the natural satellite (red) and surface data sets (green). Most GCMs differ substantially from the natural AR value, but some GCMs are better than others. Models that showed reasonable agreement were NCAR1, NCAR2, MIROC3, MRI, and MIUB. Others may be less useful as test-beds of the natural system. These results indicate a subset of models will be more realistic, and a consensus of models will give inferior results.

5 Greenhouse gas and other forcings

We have not yet excluded a role for CO_2 in the system dynamics, or shown the effects of CO_2 varying independently due to human emissions. That the atmosphere has failed to warm since 2001, over the same ten year period that atmospheric carbon dioxide concentrations have increased by 5% (which

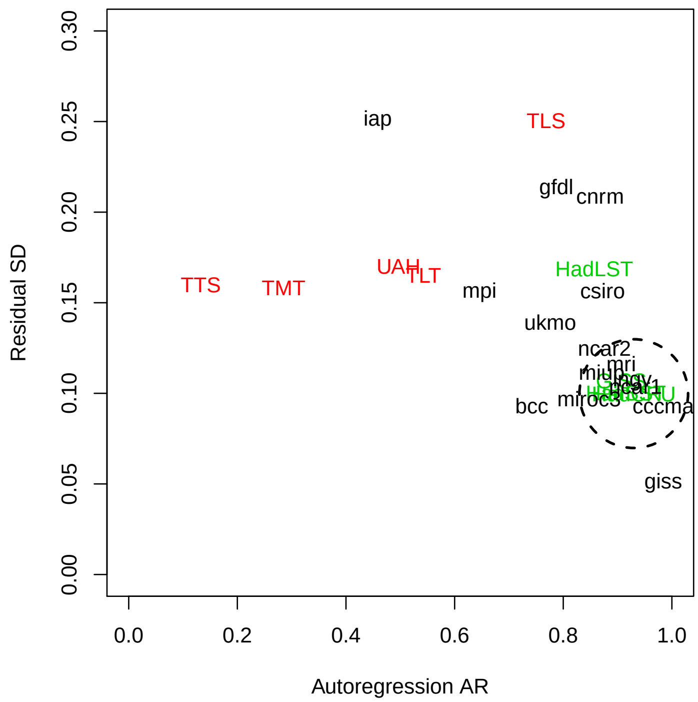

Figure 13: The relative location of GCMs (black), satellite temperature (red) and surface temperature (green) by the AR and SD parameters. The dashed circle encloses the most realistic models.

	AR	sd1	SD	tau
bcc	0.7421	0.0036	0.0930	3.88
cccma	0.9842	0.0002	0.0920	63.20
cnrm	0.8680	0.0019	0.2076	7.58
csiro	0.8724	0.0021	0.1567	7.84
gfdl	0.7873	0.0031	0.2128	4.70
giss	0.9842	0.0002	0.0505	63.12
iap	0.4585	0.0055	0.2509	1.85
ingv	0.9273	0.0012	0.1069	13.76
miroc3	0.8476	0.0020	0.0969	6.56
miub	0.8709	0.0019	0.1116	7.74
mpi	0.6458	0.0042	0.1557	2.82
mri	0.9068	0.0012	0.1165	10.73
ncar1	0.9330	0.0012	0.1039	14.92
ncar2	0.8758	0.0025	0.1247	8.05
ukmo	0.7759	0.0030	0.1393	4.46

Table 4: Estimates of the AR coefficients and SD of general circulation models (GCMs)

represents nearly one quarter of all human emissions of carbon dioxide that have occurred since 1751), suggests that the efficacy of the greenhouse gas forcing may be lower than conventionally thought. The accumulative model explains reduced effects from greenhouse gas forcing relative to solar forcing.

Atmosphere, surface and deep ocean are forced by longwave, shortwave, and geothermal forcings respectively; x, y and z with forcing S_x, S_y and S_z respectively form a matrix recurrence equation. The eigenvalues of the matrix are 0.9997, 0.86 and 0.49, equivalent to intrinsic gains or characteristic

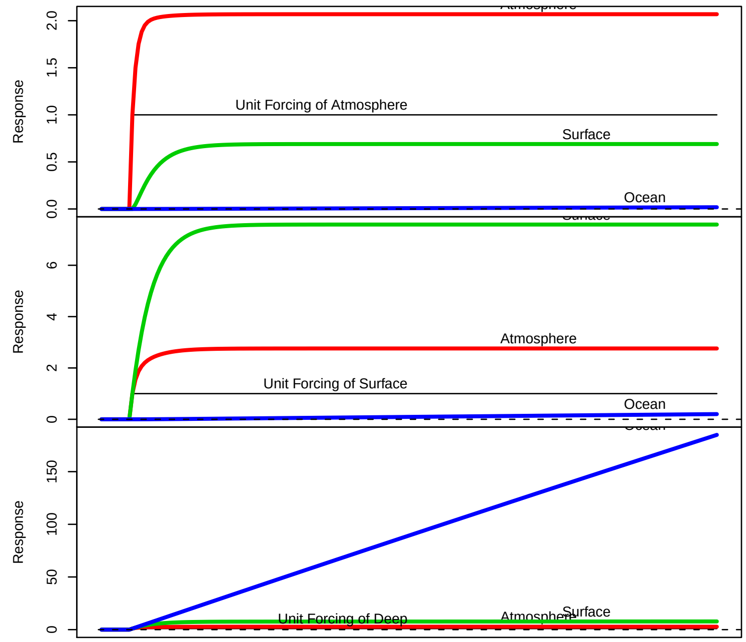

Figure 14: Response to a step forcing (black) in each of the three components: (red) atmosphere, (green) surface and (blue) deep ocean. The step function acts on each component: atmosphere, surface and deep components in the upper, middle and lower panels respectively.

rise times of 3300, 7.1 and 2.0 years respectively.

$$\begin{bmatrix} x_i \\ y_i \\ z_i \end{bmatrix} = \begin{bmatrix} 0.5 & 0.05 & 0 \\ 0.05 & 0.9 & 0.00015 \\ 0 & 0.00015 & 0.9997 \end{bmatrix} \begin{bmatrix} x_{i-1} \\ y_{i-1} \\ z_{i-1} \end{bmatrix} + \begin{bmatrix} S_x \\ S_y \\ S_z \end{bmatrix} \tag{8}$$

Fig. 14 shows 200 year simulations of the recurrence matrix with step forcing of each level in turn. The range of the responses on the Y axes to an similar step forcing varies by orders of magnitude between atmosphere (x - red), surface (y - green) and deep ocean (z - blue).

Forcing of the atmosphere reaches an equilibrium value of two (as $a = 0.5$), the surface reaches 0.5 and the deep ocean component is virtually unchanged. Unit forcing of the surface stabilizes at 8 (as $a = 0.86$) while the atmosphere rises to its previous equilibrium value of two. The deep ocean rises slightly. Unit forcing of the deepest component causes the surface and atmospheric components to respond to their equilibrium values and the deep ocean to increase to extremely high levels (as τ is large).

The system can be visualized as a downward energy cascade with upward losses. Forcing at the atmospheric, low AR, open end of the cascade, affects deeper components only after losses. In contrast, forcing of deeper components pushes shallower components to their peak equilibrium response, as the energy moves upward through the cascade. The net result in the example above is an order of magnitude difference in the effect of a unit forcing at atmosphere and surface of 0.5 and 8 units respectively.

The off-diagonal terms in the matrix determine the attenuation, and they are quite uncertain. In particular, the uncertainty of the energy flows across the thermocline is high Wigley [2005] and has recently been estimated at $2x10^{-6}m^2/s$ or $0.75m^2/year$, 50 times less than the accepted value used in most climate models Douglass et al. [2006a], resulting in a significant overestimate of net human forcing Hansen et al. [2011].

The model suggests attenuation of forcing originating in the atmosphere at the surface, and then again at a deeper ocean level. Thus, it is not necessarily the case that warming of the atmosphere by greenhouse gasses would warm the surface or the deep ocean greatly.

6 Discussion

The accumulation theory is supported by a range of evidence. Accumulated solar irradiance has a extremely high (R2=0.7) correlation with global temperature since 1950, with an excellent fit to the 11-year solar cycle and trend, but uncorrelated with direct solar radiation (Figs. 4 to 7). The only free variable in the model is the equilibrium value, determined as 1365.9 W/m^2, resulting in a solar forcing averaging $0.18W/m^2$ at the top-of-atmosphere over the period since 1950. Solar irradiance at TOA is above average for the period Lean [2001], Usoskin et al. [2003], Solanki et al. [2004]. These results are also consistent with previous phenomenological studies attributing more than half of the global temperature change since 1900 Scafetta and West [2007] and 60% of the change since the 1970's Scafetta [2009, 2010a] to natural climate oscillations.

Furthermore, the linearity of the spectral frequency plot shows that accumulation is the dominant mechanism of climate change (Fig. 1). There may be a limit to the range of temperature swings at around 22,000 years, suggesting a characteristic decay time of 3500 years from the $2\pi\tau$ bandwidth relationship. It is both surprising and compelling, that annual temperature variance is sufficient to represent global temperature dynamics over these scales, with short characteristic decay times and lags arising from the graduated mass density of the atmosphere.

The conventional view is that changes in human-caused emissions of greenhouse gases, aerosols and surface albedo cause 20th century warming Duffy et al. [2009]. These same factors support the amplification that cause glacial-interglacial transitions and paleoclimate temperature variation Hansen et al. [2011]. In the alternative theory developed here, changes in temperature due to accumulation of solar heat causes changes in greenhouse gasses and surface albedo.

The discussion is structured around the main objections to a large solar influence after Duffy et.al. (2009).

The first view (H_0) is that changes in solar radiation have little effect on global temperature, and that changes in greenhouse gas concentrations explain the majority of contemporary and paleoclimatic variability. The second view (H_a) is that solar variation has a significant effect, greater than 50% with the residual trend due to other factors such as urban heat island effect, natural cycles, cloud albedo changes or greenhouse gasses. Note that the H_a does not exclude the possibility of observable effects from rising greenhouse gas concentrations, whereas H_0 excludes the possibility of strong solar effects.

The first objection to H_a is that the amplitude of the 11 year solar cycle is no more than a few hundredths of a degree. The amplitude would be much larger if solar sensitivity is high North et al. [2004]. We have shown an 11 year cycle with magnitude of more than 0.1C using the accumulated solar variable (Fig. 7). This argument incorrectly assumes that the solar effect must be fast and direct, not slowly integrated.

Have variations in TSI have been too small to have contributed to global warming over the last few solar cycles Foukal et al. [2006]? The accumulative model only requires that the Sun's brightness be greater than average over the period, and indeed there has been a long term increase in solar flux that peaked in 1986 with the Grand Solar Maximum Usoskin et al. [2003], Solanki et al. [2004], Lockwood et al. [2009]. We showed that accumulated surplus solar irradiation can explain most of the increase in temperature over the period.

Is the hypothesis that solar variability is the dominant climate effect a 'non-solution to a non-problem', as direct forcing by albedo, ice extent and vegetation, aerosols, and greenhouse gasses adequately explain temperature change Duffy et al. [2009]? The accumulation theory is more parsimonious, explaining the main features of 20th century warming and the magnitude of variations from one to one million years with a simple, single variable model.

Positive feedbacks may help to trap heat Dessler [2010], but the notion of 'equilibrium climate sensitivity' is largely unnecessary as the accumulative response is not associated with a variety of materials with specific properties and lags.

The H_0 does not exclude an exotic solar influence on climate by regulating more energetic process, such as the influence of gamma ray flux on cloud albedo Svensmark [2007]. Duffy et.al. (2009) find exotic solar effects unlikely because observed global warming requires a forcing of $0.3W/m^2$ at top-of-atmosphere evenly distributed over the ocean and land. We have shown a similar net forcing from accumulated solar anomaly. Slow equilibration is not an exotic mechanism.

Has the effect of CO_2 been confirmed by spectral studies of the upper atmosphere? These measurements are subject to large uncertainties and contrary to Harries (2001), recent data show that the expected strong CO_2 absorption band in the 700 to 800 cm^{-1} band does not appear in the observations of the difference radiance range between 1970 and 1997 Lu [2010]. Moreover, and the H_a does not preclude some noticeable GHG effects of this nature.

The H_a contradicts the strong effect of GHGs shown by extensive GCM simulations IPCC [2007]. Climate models underestimate the observed response to solar forcing Stott et al. [2003], and poorly parametrise ocean mixing parameters overstating the net human-made forcing Hansen et al. [2011]. We have shown both poor parameterization in GCMs, and that surface response to atmospheric forcing can be an order of magnitude lower than the same intensity of surface forcing (Fig, 12) due to energy losses down through the system.

It could also be said that GCMs already incorporate the slow equilibration effect though coupled ocean-atmosphere simulations. However, many of the parameters in GCMs are virtually unmeasured and involve considerable uncertainty. The range of AR and SD values derived from a representative set of GCM simulations (Fig. 13) is large and generally unrealistic.

Another objection from Duffy et.al. (2009) is that dominant forcing by greenhouse gasses already explains the atmosphere of Venus, cooling of the stratosphere, and other phenomena IPCC [2007]. Firstly, the observable fingerprints of GHGs may coexist with the H_a, and secondly most atmospheric phenomena are subject to confounding influences e.g. ozone decline has also caused stratospheric cooling.

Duffy et.al. (2009) deprecates the 'new science' required to explain phenomenological findings of high solar influence. All theories start from a desire to explain phenomena, constrained by fundamental physics. The accumulation model is a physically-justified energy balance models with physical parameters including the mass and density of the atmosphere and ocean. The basis of the theory, like all known physics, is the conservation of energy and the appropriate relationship between radiative forcings and the accumulation of heat.

The three dimensional atmosphere/surface/ocean recurrence matrix model may be said to be simplistic. Among the advantages of the approach is freedom to incorporate additional, say, stratospheric, or land/sea components. The model thus satisfies one of the main requirements of a rigorous forecasting procedure Green and Armstrong [2008] being only as complex as necessary, representing appropriate functional relationships and system decomposition. Its symmetric tridiagonal matrix form is particularly useful for computationally intensive operations such as Monte Carlo sensitivity testing. The study of emergent behaviour of matrix structures would be worthwhile, as would the wider use of control system theory.

7 Conclusions

Contrary to the consensus view, the historic temperature data displays high sensitivity to solar variations when related by slow equilibration dynamics. A variety of results suggest that inappropriate specification of the relationship between forcing and temperature may be responsible for previous studies finding low correlations of solar variation to temperature. The accumulation model is a feasible alternative mechanism for explaining both paleoclimatic temperature variability and contemporary warming without recourse to increases in heat-trapping gases produced by human activities. There are no valid grounds to dismiss the potential domination of 20th century warming by solar variations.

8 Appendix 1. Datasets and Software

The sources of data and analysis were as follows:

The data were analysed with the R statistical language (`http://www.r-project.org/`) with the supplied ARIMA function. The code is available on request from the author.

The EPICA ice core provides was an 800,000 year temperature record and was downloaded from the National Climate Data Center (`ftp://ftp.ncdc.noaa.gov/pub/data/paleo/icecore/antarctica/vostok/deutnat.txt`) then averaged into 1000 year steps.

Temperature variations over the last two millennia were from reconstructions using proxy data by Loehle Loehle [2007] (http://www.ncasi.org/publications/Detail.aspx?id=3025) and by Moberg Moberg et al. [2005] (http://www.ncdc.noaa.gov/paleo/globalwarming/moberg.html). These data were aggregated to 20 year steps.

The annual global temperature data over the last 150 years (combined HadCRUT , land LST, and sea SST) were downloaded from the Climate Research Unit (http://www.cru.uea.ac.uk/cru/data/temperature/hadcrut3vgl.txt).

The monthly satellite global temperature data for the troposphere temperature records (UAH) were downloaded from Remote Sensing Systems and University of Alabama Hunstville (http://vortex.nsstc.uah.edu/data/msu/t2lt/uahncdc.lt) and troposphere levels (TST, TMT, TLT) and from Remote Sensing Systems (http://www.ssmi.com/msu/msu_data_description.html).

The solar irradiance data were downloaded from the KNMI Climate Explorer (http://climexp.knmi.nl; MONTHLY MEAN TSI: Lean GRL 2000). Monthly sun spot numbers were downloaded from the National Aeronautics and Space Administration (http://solarscience.msfc.nasa.gov/greenwch/spot_num.txt).

Annual solar and volcanic forcing, aerosols and well-mixed greenhouse gases were downloaded from the NASA, Goddard Institute of Space Sciences (http://data.giss.nasa.gov/modelforce/RadF.txt).

The simulations of GCMs were downloaded from KNMI and labled according to parent organization as indicated (`http://climexp.knmi.nl`):

BCC: `itas_bcc_cm1_20c3m_0-360E_-90-90N_n_++a.txt`

CCCMA: `itas_cccma_cgcm3_1_t63_20c3m_0-360E_-90-90N_na.txt`

CNM: `itas_cnrm_cm3_20c3m_0-360E_-90-90N_na.txt`

CSIRO: `itas_csiro_mk3_5_20c3m_0-360E_-90-90N_n_++a.txt`

GFDL: `itas_gfdl_cm2_1_20c3m_0-360E_-90-90N_n_++a.txt`

GISS: `itas_giss_aom_20c3m_0-360E_-90-90N_n_++a.txt`

NCAR2: `itas_ncar2_pcm1_20c3m_0-360E_-90-90N_n_++a.txt`

UKMO: `itas_ukmo_hadcm3_20c3m_0-360E_-90-90N_n_++a.txt`

NCAR1: `itas_ncar1_ccsm3_0_20c3m_0-360E_-90-90N_n_++a.txt`

MRI: `itas_mri_cgcm2_3_2a_20c3m_0-360E_-90-90N_n_++a.txt`

MPI: `itas_mpi_echam5_20c3m_0-360E_-90-90N_n_++a.txt`

MIUB: `itas_miub_echo_g_20c3m_0-360E_-90-90N_n_++a.txt`

MIROC3: `itas_miroc3_2_medres_20c3m_0-360E_-90-90N_n_++a.txt`

INGV: `itas_ingv_echam4_20c3m_0-360E_-90-90N_na.txt`

IAP: `itas_iap_fgoals1_0_g_20c3m_0-360E_-90-90N_n_++a.txt`

9 acknowledgements

In working on the problem here, I have had the loyal support of my friend and colleague Anthony Cox, and I am indebted to Demetris Koutsoyiannis

for a review of a preliminary draft.

10 acknowledgements

References

Michael Beenstock and Yaniv Reingewertz. Polynomial Cointegration Tests of the Anthropogenic Theory of Global Warming. *Pre-print*, pages 1–20, 2010. URL http://economics.huji.ac.il/facultye/beenstock/Nature_Paper091209.pdf.

Frida A.M. Bender, Annica M. L. Ekman, and Henning Rodhe. Response to the eruption of Mount Pinatubo in relation to climate sensitivity in the CMIP3 models. *Climate Dynamics*, 35(5):875–886, March 2010. ISSN 0930-7575. doi: 10.1007/s00382-010-0777-3. URL http://www.springerlink.com/index/10.1007/s00382-010-0777-3.

Trevor Breusch and Farshid Vahid. Global Temperature Trends. *Working Papers in Economics and Econometrics*, (495), 2008. URL http://ideas.repec.org/p/acb/cbeeco/2008-495.html.

A E Dessler. A determination of the cloud feedback from climate variations over the past decade. *Science (New York, N.Y.)*, 330(6010):1523–7, December 2010. ISSN 1095-9203. doi: 10.1126/science.1192546. URL http://www.sciencemag.org/content/330/6010/1523.abstract.

D. H. Douglass, R. S. Knox, B. D. Pearson, and a. Clark. Thermocline flux exchange during the Pinatubo event. *Geophysical Research Letters*, 33(19):1–5, October 2006a. ISSN 0094-8276. doi: 10.1029/2006GL026355. URL `http://www.agu.org/pubs/crossref/2006/2006GL026355.shtml`.

D. H. Douglass, R. S. Knox, B. D. Pearson, and A. Clark. Thermocline flux exchange during the Pinatubo event. *Geophysical Research Letters*, 33(19):L19711, October 2006b. ISSN 0094-8276. doi: 10.1029/2006GL026355. URL `http://www.agu.org/pubs/crossref/2006/2006GL026355.shtml`.

David H Douglass and B David Clader. Climate sensitivity of the Earth to solar irradiance. *Geophys. Res. Lett.*, 29, 2002. URL `http://dx.doi.org/10.1029/2002GL015345`.

David H Douglass and Robert S Knox. Climate forcing by the volcanic eruption of Mount Pinatubo. *Geophys. Res. Lett.*, 32, 2005. URL `http://dx.doi.org/10.1029/2004GL022119`.

David H. Douglass and Robert S. Knox. Ocean heat content and Earth's radiation imbalance. *Physics Letters A*, 373(36):3296–3300, August 2009. ISSN 03759601. doi: 10.1016/j.physleta.2009.07.023. URL `http://adsabs.harvard.edu/abs/2009PhLA..373.3296D`.

David H. Douglass, John R. Christy, Benjamin D. Pearson, and S. Fred Singer. A comparison of tropical temperature trends with model predictions. *International Journal of Climatology*, 28(13):1693–1701, November

2008. ISSN 08998418. doi: 10.1002/joc.1651. URL http://doi.wiley.com/10.1002/joc.1651.

Phillip B. Duffy, Benjamin D. Santer, and Tom M.L. Wigley. Solar variability does not explain late-20th-century warming. *Physics Today*, 62(1), 2009. URL http://dx.doi.org/10.1063/1.3074263.

G Foster, J D Annan, P D Jones, M E Mann, B Mullan, J Renwick, J Salinger, G A Schmidt, and K E Trenberth. Comment on "Influence of the Southern Oscillation on tropospheric temperature". *Journal of Geophysical Research*, 2009.

P Foukal, C Fröhlich, H Spruit, and T M L Wigley. Variations in solar luminosity and their effect on the Earth's climate. *Nature*, 443(7108): 161–6, September 2006. ISSN 1476-4687. doi: 10.1038/nature05072. URL http://dx.doi.org/10.1038/nature05072.

K C Green and J S Armstrong. Global Warming: Forecasts by scientists vs. scientific forecasts. *Energy & Environment Environment*, 18(7 +8): 997–1021, 2008.

James Hansen, Makiko Sato, Pushker Kharecha, and Karina von Schuckmann. Earth's Energy Imbalance and Implications. *eprint arXiv:1105.1140*, page 52, May 2011. URL http://arxiv.org/abs/1105.1140.

Sherwood B Idso. CO2-induced global warming : a skeptic\'s view of potential climate change. *Climate Research*, 10:69–82, 1998.

IPCC. *Climate Change 2007: The Physical Science Basis. Contribution of Working Group I to the Fourth Assessment Report of the Intergovernmental Panel on Climate Change*. Cambridge University Press 32 Avenue of the Americas, New York, NY 10013-2473, USA, 2007.

R S Knox and D H Douglass. Recent energy balance of Earth. *Online*, 1(3): 2–4, 2010. doi: 10.4236/ijg2010.00000.

D Koutsoyiannis and T A Cohn. The Hurst phenomenon and climate. In *Geophysical Research Abstracts*, volume 10, Vienna, 2008. Eurpopean Geosciences Union. URL `http://www.itia.ntua.gr/en/docinfo/849/`.

D. Koutsoyiannis, A. Efstratiadis, N. Mamassis, and A. Christofides. On the credibility of climate predictions. *Hydrological Sciences Journal*, 53 (4):671–684, August 2008. ISSN 0262-6667. doi: 10.1623/hysj.53.4.671. URL `http://www.informaworld.com/10.1623/hysj.53.4.671`.

J Lean and D Rind. Sun-climate connections. Earth's response to a variable Sun. *Science*, 292(5515), 2001. URL `http://www.ncbi.nlm.nih.gov/entrez/query.fcgi?cmd=Retrieve&db=PubMed&dopt=Citation&list_uids=11305317`.

J. L. Lean. Solar irradiance and climate forcing in the near future. *Geophysical Research Letters*, 28(21):4119, 2001. ISSN 0094-8276. doi: 10.1029/2001GL013969. URL `http://www.agu.org/pubs/crossref/2001/2001GL013969.shtml`.

Judith L. Lean and David H. Rind. How natural and anthropogenic influences alter global and regional surface temperatures: 1889 to 2006. *Geo-*

physical Research Letters, 35(18):L18701, September 2008. ISSN 0094-8276. doi: 10.1029/2008GL034864. URL `http://www.agu.org/pubs/crossref/2008/2008GL034864.shtml`.

Richard S. Lindzen and Yong-Sang Choi. On the determination of climate feedbacks from ERBE data. *Geophysical Research Letters*, 36(16):L16705, August 2009. ISSN 0094-8276. doi: 10.1029/2009GL039628. URL `http://www.agu.org/pubs/crossref/2009/2009GL039628.shtml`.

M. Lockwood, A. P. Rouillard, and I. D. Finch. The rise and fall of open solar flux dueing the current grand solar maximum. *The Astrophysical Journal*, 700(2):937–944, August 2009. ISSN 0004-637X. doi: 10.1088/0004-637X/700/2/937. URL `http://iopscience.iop.org/0004-637X/700/2/937`.

Mike Lockwood and Claus Fröhlich. Recent oppositely directed trends in solar climate forcings and the global mean surface air temperature. II. Different reconstructions of the total solar irradiance variation and dependence on response time scale. *Proceedings of the Royal Society A: Mathematical, Physical and Engineering Sciences*, 464(2094):1367–1385, June 2008. ISSN 1364-5021. doi: 10.1098/rspa.2007.0347. URL `http://rspa.royalsocietypublishing.org/cgi/content/abstract/464/2094/1367`.

C Loehle. A 2000-year global temperature reconstruction based on non-treering proxies. *Energy & Environment*, 19(1):93–100, 2007.

Craig Loehle. Cooling of the global ocean since 2003. *Energy & environment*, 20(1-2):101–104, 2009. ISSN 0958-305X. URL http://cat.inist.fr/?aModele=afficheN&cpsidt=21332496.

Q.B. Lu. What is the Major Culprit for Global Warming: CFCs or CO2? *Journal of Cosmology*, 8:1846–1862, 2010. URL http://www.probeinternational.org/Qing-BinLuonCFCsandGlobalCooling.pdf.

J. D. McLean, C. R. de Freitas, and R. M. Carter. Influence of the Southern Oscillation on tropospheric temperature. *Journal of Geophysical Research*, 114(D14):D14104, July 2009. ISSN 0148-0227. doi: 10.1029/2008JD011637. URL http://www.agu.org/pubs/crossref/2009/2008JD011637.shtml.

Anders Moberg, Dmitry M Sonechkin, Karin Holmgren, Nina M Datsenko, and Wibjorn Karlen. Highly variable Northern Hemisphere temperatures reconstructed from low- and high-resolution proxy data. *Nature*, 433(7026):613–617, 2005. URL http://dx.doi.org/10.1038/nature03265.

R Muscheler, F Joos, J Beer, S Muller, M Vonmoos, and I Snowball. Solar activity during the last 1000yr inferred from radionuclide records. *Quaternary Science Reviews*, 26(1-2):82–97, January 2007. ISSN 02773791. doi: 10.1016/j.quascirev.2006.07.012. URL http://dx.doi.org/10.1016/j.quascirev.2006.07.012.

G. R. North, Q. Wu, and M. J. Stevens. Detecting the 11-year Solar Cycle in the Surface Temperature Field. *Solar Variability and its Effects on Climate. Geophysical Monograph 141*, 2004. URL http://adsabs.harvard.edu/abs/2004GMS...141..251N.

Gerard Roe. Feedbacks, Timescales, and Seeing Red. *Annual Review of Earth and Planetary Sciences*, 37(1):93–115, May 2009. ISSN 0084-6597. doi: 10.1146/annurev.earth.061008.134734. URL `http://www.annualreviews.org/doi/abs/10.1146/annurev.earth.061008.134734?journalCode=earth`.

B D Santer, P W Thorne, L Haimberger, K E Taylor, T M L Wigley, J R Lanzante, S Solomon, M Free, P J Gleckler, P D Jones, T R Karl, S A Klein, C Mears, D Nychka, G A Schmidt, S C Sherwood, and F J Wentz. Consistency of modelled and observed temperature trends in the tropical troposphere. *International Journal of Climatology*, 28:1703–1722, 2008.

N. Scafetta and B. J. West. Phenomenological reconstructions of the solar signature in the Northern Hemisphere surface temperature records since 1600. *Journal of Geophysical Research*, 112(D24):D24S03, November 2007. ISSN 0148-0227. doi: 10.1029/2007JD008437. URL `http://www.agu.org/pubs/crossref/2007/2007JD008437.shtml`.

Nicola Scafetta. Empirical analysis of the solar contribution to global mean air surface temperature change. *Journal of Atmospheric and Solar-Terrestrial Physics*, 71(17-18):1916–1923, December 2009. ISSN 13646826. doi: 10.1016/j.jastp.2009.07.007. URL `http://arxiv.org/abs/0912.4319`.

Nicola Scafetta. Empirical evidence for a celestial origin of the climate oscillations and its implications. *Journal of Atmospheric and Solar-*

Terrestrial Physics, 72(13):951–970, August 2010a. ISSN 13646826. doi: 10.1016/j.jastp.2010.04.015. URL `http://arxiv.org/abs/1005.4639`.

Nicola Scafetta. Empirical evidence for a celestial origin of the climate oscillations and its implications. *Journal of Atmospheric and Solar-Terrestrial Physics*, 72(13):951–970, August 2010b. ISSN 13646826. doi: 10.1016/j.jastp.2010.04.015. URL `http://dx.doi.org/10.1016/j.jastp.2010.04.015`.

Nicola Scafetta, Bruce J. West, Benjamin R. Jordan, Philip Duffy, Benjamin Santer, and Tom Wigley. Interpretations of climate-change data. *Physics Today*, 62(11):8–12, November 2009. URL `http://link.aip.org/link/?PTO/62/8/2`.

Nir J. Shaviv. Using the oceans as a calorimeter to quantify the solar radiative forcing. *Journal of Geophysical Research*, 113(A11):A11101, November 2008. ISSN 0148-0227. doi: 10.1029/2007JA012989. URL `http://www.agu.org/pubs/crossref/2008/2007JA012989.shtml`.

S K Solanki, I G Usoskin, B Kromer, M Schüssler, and J Beer. Unusual activity of the Sun during recent decades compared to the previous 11,000 years. *Nature*, 431(7012):1084–7, October 2004. ISSN 1476-4687. doi: 10.1038/nature02995. URL `http://dx.doi.org/10.1038/nature02995`.

R W Spencer and W D Braswell. Potential biases in cloud feedback diagnosis: A simple model demonstration. *J Clinate*, 21:5624–5628., 2008.

Roy W. Spencer and William D. Braswell. On the diagnosis of radiative feedback in the presence of unknown radiative forcing. *Journal* *of Geophysical Research*, 115(D16):D16109, August 2010. ISSN 0148-0227. doi: 10.1029/2009JD013371. URL `http://www.agu.org/pubs/crossref/2010/2009JD013371.shtml`.

David I. Stern. A Three-Layer Atmosphere-Ocean Time Series Model of Global Climate Change. *Unpublished*, 2005. URL `http://ideas.repec.org/p/rpi/rpiwpe/0510.html`.

David R B Stockwell. *Ecological Niche Modeling: Ecoinformatics in Application to Biodiversity*, chapter 7. CRC Press, 2006.

David R. B. Stockwell and Anthony Cox. Comment on "Influence of the Southern Oscillation on tropospheric temperature" by J. D. McLean, C. R. de Freitas, and R. M. Carter. August 2009. URL `http://arxiv.org/abs/0908.1828`.

Peter a. Stott, Gareth S. Jones, and John F. B. Mitchell. Do Models Underestimate the Solar Contribution to Recent Climate Change? *Journal of Climate*, 16(24):4079, 2003. ISSN 0894-8755. doi: 10.1175/1520-0442(2003)016<4079:DMUTSC>2.0.CO;2. URL `http://journals.ametsoc.org/doi/abs/10.1175/1520-0442(2003)016<4079:DMUTSC>2.0.CO;2`.

Allen Stubberud, Ivan Williams, and Joseph DiStefano. *Schaum's Outline of Feedback and Control Systems (Schaum's)*. McGraw-Hill, 1994. ISBN 0070170525. URL `http://www.amazon.com/Schaums-Outline-Feedback-Control-Systems/dp/0070170525`.

Henrik Svensmark. Cosmoclimatology: a new theory emerges. *Astronomy & Geophysics*, 48(1):1.18–1.24, February 2007. ISSN 1366-8781. doi: 10.

1111/j.1468-4004.2007.48118.x. URL http://doi.wiley.com/10.1111/j.1468-4004.2007.48118.x.

R. S. J. Tol and P. Vellinga. Climate Change, the Enhanced Greenhouse Effect and the Influence of the Sun: A Statistical Analysis. *Theoretical and Applied Climatology*, 61(1-2):1–7, November 1998. ISSN 0177-798X. doi: 10.1007/s007040050046. URL http://www.springerlink.com/content/jtfna97vadpeqje0/.

Ilya Usoskin, Sami Solanki, Manfred Schüssler, Kalevi Mursula, and Katja Alanko. Millennium-Scale Sunspot Number Reconstruction: Evidence for an Unusually Active Sun since the 1940s. *Physical Review Letters*, 91 (21):211101, November 2003. ISSN 0031-9007. doi: 10.1103/PhysRevLett.91.211101. URL http://link.aps.org/doi/10.1103/PhysRevLett.91.211101.

D Vjushin, R B Govindan, S Brenner, A Bunde, S Havlin, and H-J Schellnhuber. Lack of scaling in global climate models. *Journal of Physics: Condensed Matter*, 14(9):2275, 2002. URL http://stacks.iop.org/0953-8984/14/i=9/a=316.

T. M. L. Wigley. Comment on âĂIJClimate forcing by the volcanic eruption of Mount PinatuboâĂİ by David H. Douglass and Robert S. Knox. *Geophysical Research Letters*, 32(20):L20709, October 2005. ISSN 0094-8276. doi: 10.1029/2005GL023312. URL http://www.agu.org/pubs/crossref/2005/2005GL023312.shtml.

J Zachos, M Pagani, L Sloan, E Thomas, and K Billups. Trends, rhythms, and aberrations in global climate 65 Ma to present. *Science (New York, N.Y.)*, 292(5517):686–93, April 2001. ISSN 0036-8075. doi: 10.1126/science.1059412. URL http://www.sciencemag.org/content/292/5517/686.abstract.